Multi-Mission Performance Optimization of a Hybrid-Electric Unmanned Aerial Vehicle

Jonathan Gladin

Anusha Harish

Dimitri Mavris
UNITED STATES OF AMERICA

jgladin3@gatech.edu, aharish9@gatech.edu, dimitri.mavris@aerospace.gatech.edu

Keywords: *Conceptual Design, Hybrid, UAV, Drone*

ABSTRACT

The US Department of Defense is interested in the development of UAV's capable of flying multiple missions with interchangeable payloads. Hybrid-electric propulsion is one solution to help enable this capability, though sizing of such vehicles poses a challenge for traditional conceptual design optimization tools. This paper discusses an optimization approach for a hybrid-electric unmanned aerial vehicle capable of performing multiple missions in various hybrid modes.

A methodology is constructed considering the potential for hybridization and for multiple missions with parameters specified for each mission. Various objective functions are considered and developed representing potentially different value functions for each type of mission. A specific application is implemented for an MQ-1B Predator class drone considering missions for long-range endurance and a shorter range all-electric quiet endurance mission with a parallel hybrid-electric configuration partially driven by batteries.

Optimal designs were found considering various objective functions and sizing constraints. Significant all-electric cruise can be achieved at current technology levels with an ~80hp electric motor drive. However, results indicate significant endurance (~10%) compromises would be required to enable the all-electric cruise application. However, more significant benefits may be possible if the battery specific energy approximately doubles from current state of art or if other architectural or mission capabilities are considered. The authors recommend that the current methodology be potentially extended to other types of benefits or missions for the Predator class ISR drone to further investigate the potential for hybrid electric in this space and to expand the analysis to other architectures such as series hybrid. The authors further recommend that operational analysis be conducted to provide more informed weighting functions for the decisions being made during the optimization process.

1.0 INTRODUCTION

Hybrid-electric propulsion is considered a promising solution to some of the challenges in the aviation industry today. While there is ongoing research in this field for commercial aircraft, a potential military application is Unmanned Aerial Vehicles (UAVs) ([2],[4],[6]). Previous studies have shown that a parallel hybrid configuration is most advantageous for UAVs in terms of range and endurance. The weight penalty in other configurations negate the benefits of the system [6].

A future research goal envisioned by the United States Department of Defense is the development of UAVs capable of performing multiple missions with interchangeable payloads [3]. Hybrid-electric propulsion could help UAVs achieve this capability. The battery on board can be used to offset fuel burn or engine weight by providing additional power. The hybrid system can also enable certain tactically advantageous operations. For example, during reconnaissance missions, the engine can be shut off or throttled down, utilizing only the electric motors, which are quieter and have reduced heat signatures. The focus of this paper is to develop a methodology to evaluate and perform conceptual design studies of hybrid electric configurations from a multi-mission perspective.

2.0 VEHICLE CONFIGURATION

2.1 Aircraft System Configuration

of the system.

First, the typical attachment point for storable weapons will be assumed to be retrofit for an ISR mission allowing attachment of removable battery packs for an all-electric endurance mission. There will be an optional wing integrated battery pack located within the inboard section of the wing. The geometry outlined in Figure 2.1-1**Błąd! Nie można odnaleźć źródła odwołania.** shows a nominal size for the UAV and not the final sized or optimized battery size layout.

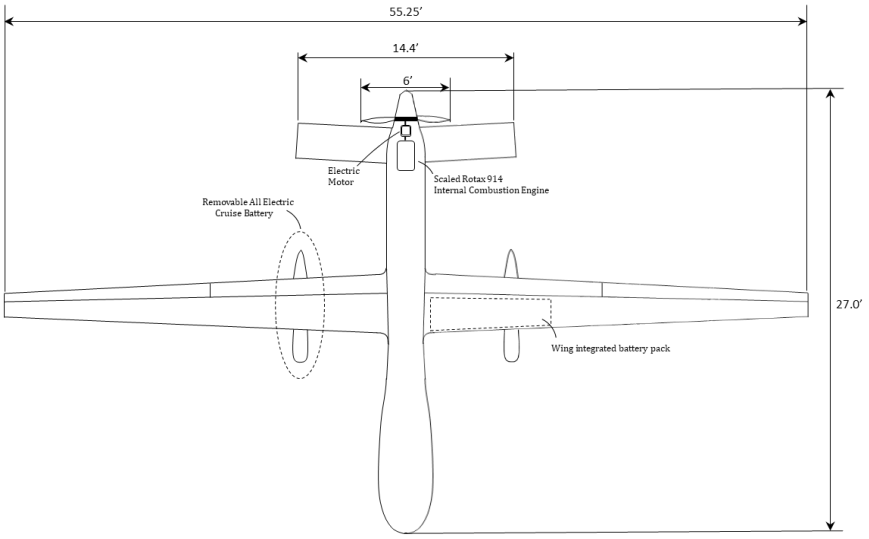

Figure 2.1-1 Hybrid-Electric UAV configuration layout based on the General Atomics Predator MQ-1 configuration

The electric motor is assumed to be on the higher RPM side of the stepper gear box of the original Rotax IC engine (gear ratio of 2.43:1). This allows for a better overall specific power for the system. This paper will not focus on the viability of the integration of the electric motor within the original Rotax design spatially, but will assume such integration is possible and consider the performance implications within the methodology developed herein.

Table 2.1-1 General configuration characteristics [8]

Aircraft Parameter	Value	Unit
MTOW	2250	lbs
Range	675	Nm
Payload	450	lbs
Wing Span	55.25	ft
Wing Area	123.2	ft^2
Max. End.	40.33	hrs
Engine Power (Rotax 914)	115 85.75	Hp kW
Cruise Speed	94	kts
Ceiling	25000	ft
Cruise Alt.	17000	ft
Fuel capacity	665	lbs

2.2 Hybrid Propulsion System Parameters

The hybrid propulsion system as shown schematically below in 2.2-1 includes energy sources, and mechanical/electrical distribution and conversion components. The power distribution is assumed to be an AC distribution system with a relatively standard bus voltage.

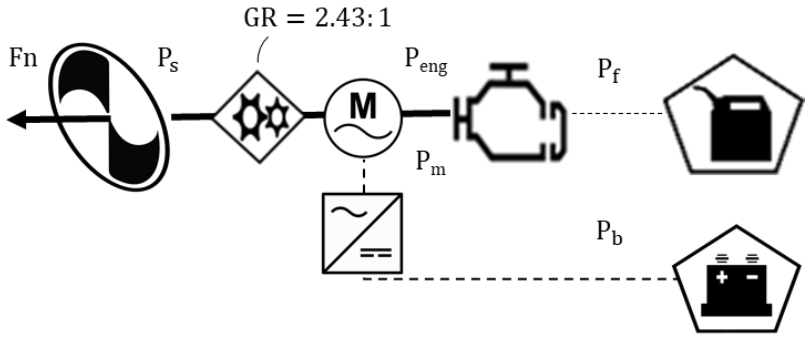

Figure 2.2-1 Parallel hybrid power train diagram with nomenclature for various power stations

The battery provides DC power to the bus system and inverter, which converts DC to AC power to drive the electric motor. The battery discharge efficiency can be defined as the ratio of DC output power to rate of discharge of chemical energy or electrical charge, as seen in eqn. 1. This efficiency represents Coulombic and resistive losses within the battery circuit itself, and varies between 80-100% for Lithium-Ion batteries.

$$\eta_b = \frac{P_b}{\dot{E}_b} \tag{1}$$

The overall electrical efficiency can be computed by including the efficiency of the cables, inverter, and electric motor as below in eqn. 2. These component efficiencies vary with overall current level, power output, and shaft RPM.

$$\eta_e = \eta_b \eta_c \eta_I \eta_M = \frac{P_m}{\dot{E}_b} \tag{2}$$

The thermal efficiency of the IC engine is defined as the rated shaft output power divided by the "fuel power" computed using the lower heating value of the fuel and its flow rate (eqn. 3). Typical efficiency values are within 20-30% for small spark-ignition IC engines.

$$\eta_{th} = \frac{P_{eng}}{\dot{m}_f h_{lhv}} \tag{3}$$

The hybridization of the propulsion system is represented by the parameter "supplied power ratio" or ϕ, defined below in eqn. 4 ϕ represents the proportion of power that is supplied to the propulsor shaft from the electric power path at the point of application of the shaft.

$$\phi = \frac{P_m}{P_s} = \frac{P_m}{P_m + P_{eng}} \tag{4}$$

Overall efficiency of the propulsion system can then be defined as follows:

$$\eta = [\phi \eta_e + (1 - \phi)\eta_{th}]\eta_{pr} \tag{5}$$

Here, η_{pr} is the stated propeller efficiency of the pusher propeller. Eqn. 5 shows that the efficiency of the system is essentially a weighted average of the two thermal conversion power paths with the supplied power ratio as the weighting parameter.

2.3 Mission Assumptions and Hybridization

The multi-mission methodology is tested by applying it to a vehicle designed for two specific missions - a maximum endurance mission, and a similar mission with a fixed range of 600 nmi and an all-electric loiter segment. As seen in 2.3-1 and 2.3-2, the missions constitute a takeoff and climb segment, during which hybridization is allowed (indicated by the supplied power ratio being greater than zero), a cruise segment, and a descent and landing segment at zero hybridization. In theory the cruise velocity can be optimized for different conditions. In this study however, that is fixed for both missions.

For mission 1, the cruise segment is at zero hybridization to allow for maximum endurance and range. The removable batteries are detached from the UAV and the internal battery is used to supply the necessary hybridization during the takeoff and climb segments.

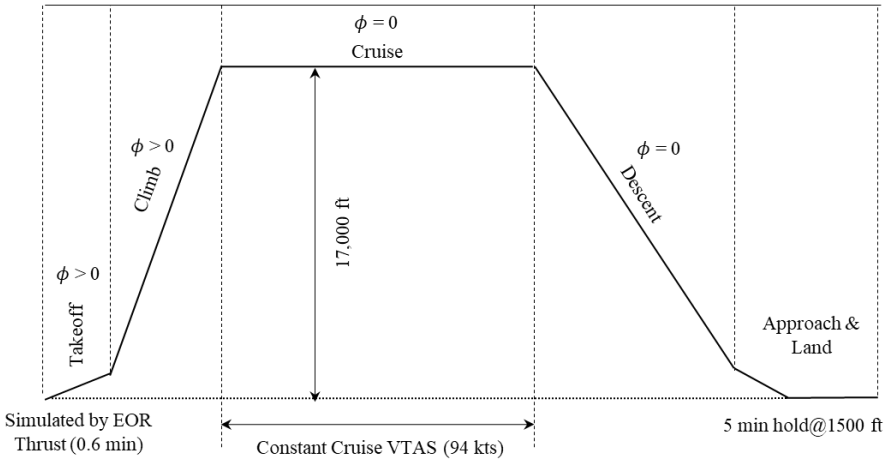

Figure 2.3-1 Diagram for maximum endurance ISR mission

Mission 2 is the all-electric loiter mission, consisting of a cruise segment with 400nm range to an intended target for the quiet loiter. The endurance for cruise segment is varied to match the available battery load which can be carried based on the gross weight limit of the airplane.

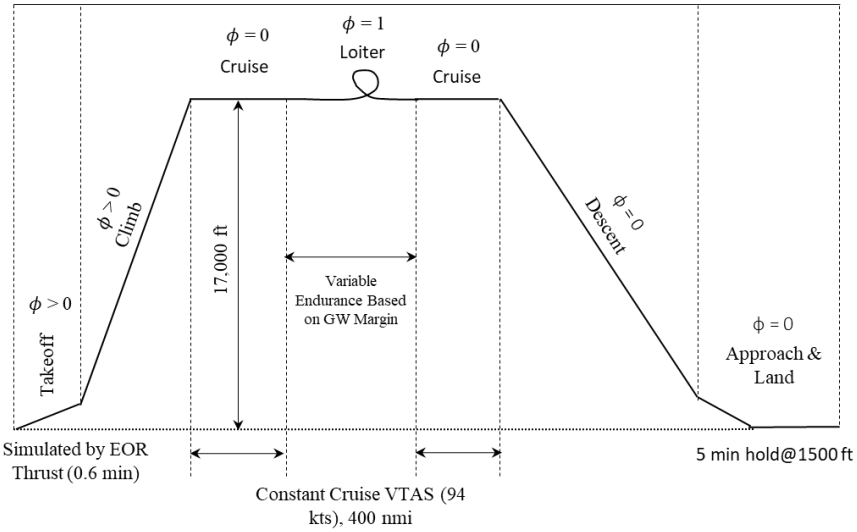

Figure 2.3-2 Diagram for all-electric loiter ISR mission

3.0 MODELING APPROACH

3.1 Propulsion

The propulsion system was modelled using a series of scalable parametric performance curves to represent IC engine and electric motor drive power, weight, and efficiency along with standard propeller performance curves.

These curves were coupled to an algorithm to match vehicle thrust demand by varying the power output (or RPM) of the propeller and gas turbine engine. Propulsion system group weights were also computed using the sizing rules outlined in the following sections.

3.1.1 Internal Combustion Engine (IC Engine)

The IC engine was modelled assuming that a similar Rotax engine can be used, scaled within the general range of similar Rotax engines (down to 80 hp). Since the engine is turbocharged and turbocharged systems can generally maintain sea-level manifold pressure up to certain altitudes, it was assumed that performance could be maintained for the common cruise altitude of 17,000 ft. These sets of curves were used to determine the fuel flow and power level at a given physical shaft RPM, which was correlated to the propeller RPM through the gear ratio of 2.43:1. The engine weight was determined by assuming a constant gravimetric specific power value of 0.69 hp/lbm (taken from the manufacturer data sheet).

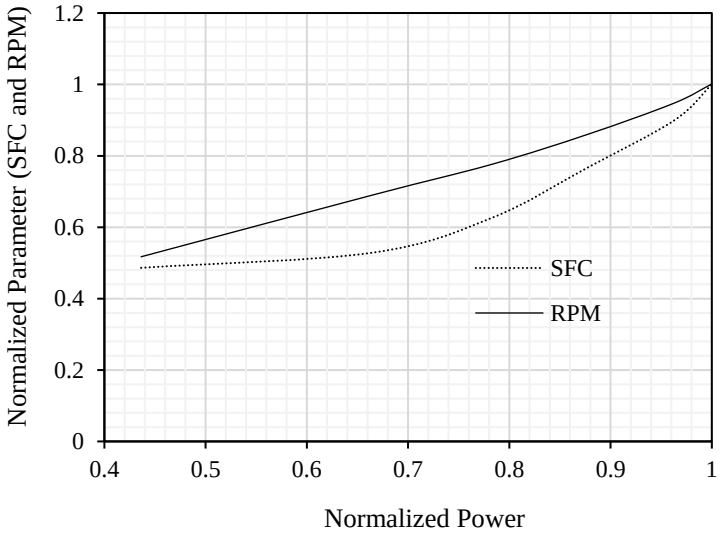

Figure 3.1.1-1 Plot of normalized RPM vs. normalized power and BSFC, all normalized relative to the sizing design point value. Adopted from Rotax 914 engine cycle sheet [9]

3.1.2 Propeller

The propeller was modelled using a Hamilton Standard map for determining approximate propeller efficiency as a function of shaft power and speed. This method correlates efficiency with ratio of the advance ratio to the power coefficient defined in eqns. 6 and 7. For each point in the mission analysis, the advance ratio J and C_p were computed, and a resulting efficiency was determined. A Hamilton Standard map was assumed to have a total activity factor of 110 per blade with a maximum integrated design Cl of 0.7.

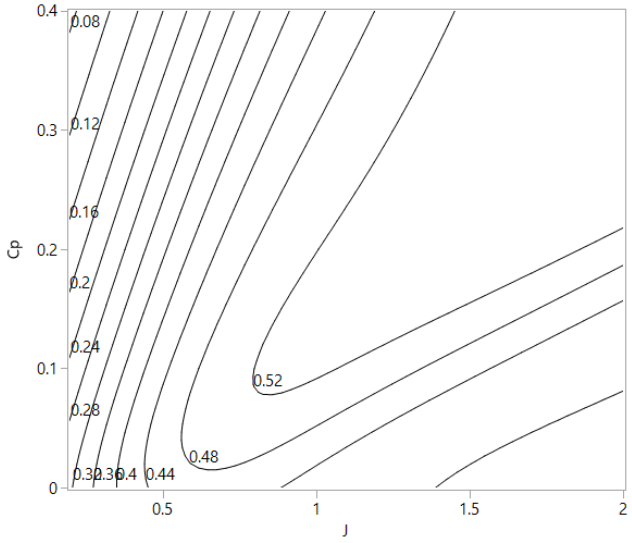

Figure 3.1.2-1 The Hamilton Standard propeller map used for the 2 bladed pusher prop.

$$V = 101.4\frac{V}{ND} \tag{6}$$

$$Cp = \frac{BHP\sigma}{2000\left(\frac{N}{1000}\right)^3\left(\frac{D}{10}\right)^5} \tag{7}$$

3.1.3 Electric Drive Train

The electric motor drive was assumed to have a constant efficiency of 93%. While in reality, the efficiency depends on RPM and shaft torque, it is assumed that its variability would not be very steep within the range of values used for this application. The specific power, however, varies significantly (~0-150 hp). A correlation was used from a prior study conducted by the authors [7]**Błąd! Nie można odnaleźć źródła odwołania.**. The trend of specific power vs. electric motor size (Figure 3.1.3-1) was created by regressing the motor maximum rated torque vs. the geometric parameter D^2L, where D is the motor diameter and L is the motor length, using data from commercial off the shelf (COTS) brushless DC motors.

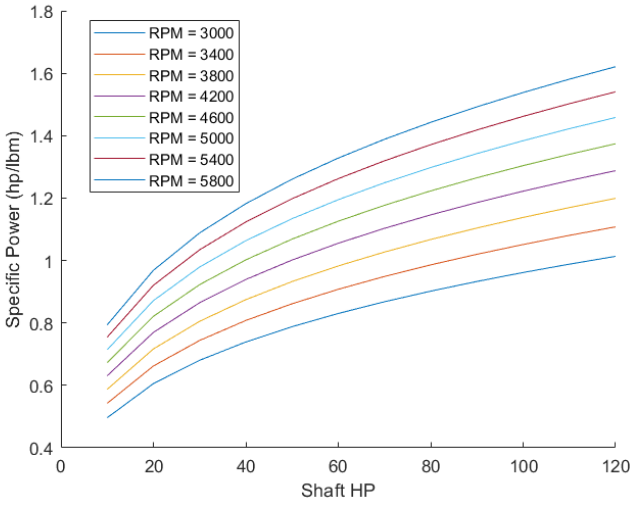

Figure 3.1.3-1 Trend of assumed electric motor specific power vs. the rated power of the electric motor. Trend lines created from correlations of COTS BLDC motors.

3.1.4 Battery

For mission 2, the battery is sized to meet the all-electric loiter segment power requirement. The battery weight is modelled as a function of its specific energy or specific power, depending on which is more critical (see eqn. 8). Based on current battery technology, the battery is assumed to be a Lithium-ion battery with specific energy and specific power of 175 Wh/kg (pack effective level including discharge limits and pack burden) and 350 W/kg respectively [1] with discharge efficiency of 95%. Discharge curves were not modelled for this work, so the DC voltage was assumed to be 540 volts (+/- 270 VDC distribution).

$$W_{batt} = \max\left(\frac{E_{batt}}{SE_{batt}}, \frac{P_{batt}}{SP_{batt}}\right) \tag{8}$$

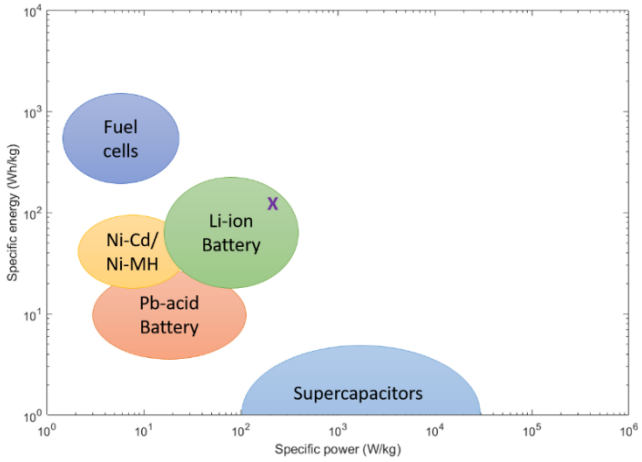

Figure 3.1.4-1 Ragone plot for electrochemical energy storage devices for current technology level (Adapted from Aravindan 2014 [1]

3.2 Aerodynamics

Since the airfoil used on the Predator UAV is proprietary, one that is expected to closely match its performance has been used. This is assumed to be the Eppler 374. The estimated aircraft drag polar is shown Figure 3.2-1.

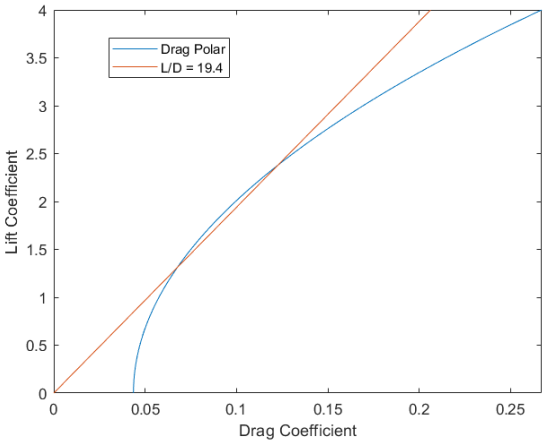

Figure 3.2-1 UAV Drag polar used for the mission analysis

The total vehicle drag is estimated as sum of zero-lift drag and induced drag. The zero-lift drag is approximated using the airfoil drag polar, and the induced drag is estimated from the lift coefficient and the wing aspect ratio using standard aerodynamics approximations. The maximum L/D of the UAV is estimated to be approximately 19.34 at a nominal cruise lift coefficient.

3.3 Weights

For a conventional aircraft, gross weight is the sum of the empty weight, payload and fuel (eqn 9). For a hybrid-electric aircraft, additional weight for the battery and electric motor need to be accounted for as demonstrated in eqn. 10.

$$\text{Conventional:} \quad W = W_{empty} + W_{payload} + W_{fuel} \tag{9}$$

$$\text{Hybrid} - \text{electric:}\ W = W'_{empty} + W_{payload} + W_{energy} \tag{10}$$

For each mission, the maximum takeoff weight and payload are kept fixed. The propulsion system (IC engine and motor) are sized for takeoff which is the most constraining requirement for the system. The fuel and battery weights are varied to meet each individual requirement.

3.3.1 Empty Weight

Since the geometry and size of the aircraft is assumed to be fixed, the structural weight is kept constant. The empty weight is updated by adding motor weight to the empty weight of the conventional aircraft, and replacing conventional IC engine weight with the weight of the resized engine as shown below in eqn 11.

$$W'_{empty} = W_{empty} - W_{ICEngine,conv} + W_{ICEngine,hybrid} + W_{electric} \tag{11}$$

3.3.2 Mission Analysis

For both missions, the energy expended during each mission segment is estimated. For each mission, the propulsion system i.e. IC engine and motor, is first sized. Then, based on the maximum takeoff weight limit, the total weight available for the energy systems (fuel and battery) is estimated. The aircraft is assumed to climb at a constant rate of climb to a cruising altitude of 17,000 ft. The battery energy required during climb is dependent on the supplied power ratio. The battery weight is then calculated based on the energy expended.

$$E_{batt} = \frac{\Phi_{climb}.P_{required}\, t_{climb}}{\eta} \tag{12}$$

3.3.3 Mission 1: Max Endurance Reconnaissance Mission

The maximum endurance for mission 1 is calculated based on the maximum available fuel. The endurance/range of the cruise segment is varied until the quantities from eqns. 13 and 14 match.

$$W_{fuel} = W_{energy} - W_{batt} \tag{13}$$

$$W_{fuel} = W_{fuel,climb} + W_{fuel,cruise} + W_{fuel,descent} \tag{14}$$

3.3.4 Mission 2: Stealth All Electric Loiter Recon Mission

While the integrated battery pack weight used during climb is calculated based on the supplied power ratio, the removable battery pack weight for the all-electric loiter is based on available battery energy. The fuel weight required for the remaining segments is first calculated. The all-electric loiter range is limited by the maximum takeoff weight.

$$W_{batt2} = W_{energy} - W_{fuel} - W_{batt1} \tag{15}$$

$$W_{fuel} = W_{fuel,climb} + W_{fuel,cruise1} + W_{fuel,cruise2} + W_{fuel,descent} \tag{16}$$

4.0 OPTIMIZATION APPROACH

4.1 General Methodology Development

The problem of designing the hybrid-electric propulsion system is formulated as a constrained multi-objective optimization problem with two sets of variables: one to describe system sizing parameters related to overall power level and degree of hybridization of power; and a second set related to the hybridization of energy (for each mission) which determine relative battery sizes used for each mission. Here, battery removability is a key necessary technical feature that allows for variable battery sizes between missions. Otherwise, the battery size and usage must be fixed for all missions.

The objective is formulated such that tradeoffs between performance metrics across the various missions are included, using a weighted sum approach where the weightings are user-defined. For each mission, individual performance metrics can be defined (range, endurance, payload, fuel burn, energy, etc.) and evaluated for different degrees of hybridization and given weightings to obtain a best overall solution (eqn. 17).

$$minimize\ F = \sum_{i=1}^{n} w_i f_i(\vec{X}, \vec{Y_i}) \tag{17}$$

Where $\vec{X}$ is a set of design variables related to overall vehicle propulsion system, $\vec{Y_i}$ is a set of design variables related to each i[th] mission, w_i is the performance metric weighting for mission 'i', and f_i is the objective function for mission 'i'. The objective function is minimized for the overall system while satisfying all system constraints.

4.2 Specific UAV Optimization Problem

4.2.1 Objective Function

The objective function is constructed by weighing possible mission metrics, which are as follows:

Mission 1:

- Total maximum endurance, total fuel consumption, total energy consumption, energy specific air range or ESAR (distance flown per unit of energy consumed), Gross weight

Mission 2:

- Total all-electric endurance, total fuel consumption, total energy consumption, ESAR, Gross weight

Fuel consumption and gross weight are usually secondary considerations in military applications since general mission capability is critical, and hence are not selected as metrics in this study. ESAR and total energy consumption both describe the overall efficiency of the aircraft. However, ESAR also accounts for the variability of mission time and range. Therefore, mission metrics selected for this study are ESAR and endurance.

Two objective functions were selected using combinations of the chosen metrics in order to emphasize various mission capabilities. The objectives for mission 1 and 2 are shown below in eqns. 18 and 18 respectively.

$$F_1 = -w_1\left(\frac{E_1}{E_{bl}}\right) - w_2\left(\frac{E_2}{E_{req}}\right) \tag{18}$$

$$F_2 = -w_1\left(\frac{ESAR_1}{ESAR_{bl}}\right) - w_2\left(\frac{E_2}{E_{req}}\right) \tag{19}$$

Where 'E' is the endurance, 'w' is the weighting factor, subscripts 'bl', '1', and '2' represent baseline configuration, missions 1 and 2 respectively, 'E_{req}' is the desired all-electric endurance, such that the second term in both equations reflect a relative percentage achieved of desired endurance. The relative values of w_1 and w_2 will determine whether the user prefers to favour mission 1 performance over that of mission 2. The second term in F_2 is exactly the same as that in F_1 since the all-electric endurance for mission 2 is considered to be more important than the ESAR.

4.2.2 Design Variables

Design variables for the propulsion system are given in eqn. 20 for the general optimization procedure. Here, PWR is the power-to-weight ratio of the system, ϕ_{des} is the supplied power ratio as defined above for the rated

design power of the system (sizing), $N_{AE,crz}$ is the shaft speed during the all-electric cruise segment, and ϕ_{climb} and ϕ_{cruise} are mission usage parameters that determine the amount of hybridization during climb and cruise respectively (which are predetermined).

$$\vec{X} = \begin{bmatrix} PWR \\ \phi_{des} \\ N_{AE,crz} \end{bmatrix}; \vec{Y} = \begin{bmatrix} \phi_{climb} & \phi_{climb} \\ 0 & \phi_{cruise} \end{bmatrix} \tag{20}$$

4.2.3 System Constraints

The following constraints are considered during the optimization:

1. Minimum power-to-weight ratio: based on the original requirements for takeoff, climb, and dash for the baseline Predator configuration.
2. Minimum electric motor power: based on the requirement for all-electric loiter or the specified climb supplied power ratio.
3. Minimum ICE power: driven by either the "all-fuel" cruise mission segment from mission 1 or maximum required power for the climb supplied power ratio
4. Maximum ICE power: constrains the maximum gas engine rated hp such that cruise part power throttle ratio is above 35%, which is the minimum allowed from available Rotax data.
5. Battery 1 usage constraints: The battery usage from the fixed battery should be equal for both missions, since the same battery is being carried for both.
6. Gross weight constraints: The aircraft gross weight cannot be greater than the maximum

Mathematically, the constraints are as follows:

$$\vec{g}\left(\vec{X},\vec{Y_i}\right) = \begin{matrix} P_{eng,min} - P_{eng} \\ P_{eng} - \frac{P_{crz}}{0.35} \\ P_{crz,AE} - P_m \\ 0.05 - PWR \\ E_{b1,1} - E_{b1,2} \\ GW - MTOW \end{matrix} \leq 0 \tag{21}$$

Where $E_{b1,1}$ is the energy used from the first battery during mission 1, and other variables have been defined previously with minimums and maximums specified.

5.0 RESULTS

5.1 Optimization Results

The optimization was carried out using a gradient based optimizer in MATLAB. Five different cases were devised varying the objective functions and the weightings as shown in Table 5.1-1 below. Interestingly, designs 1-3 exhibit similar mission 2 performance although the three cases have different values for w_2. Since the maximum weight for the airplane is set to 2250 lbs with a minimum all-electric cruise power requirement of ~71 hp, the total all-electric cruise endurance is capped at 0.458 hrs (27.5 min). However, the difference between these designs lie in the supplied power ratio usage variables and resulting battery sizes. For design 1, the optimizer finds a local optimum that has a smaller removable battery size and a very heavy fixed wing integrated battery. Due to the heavy fixed battery, higher supplied power ratio is required during the climb segment. This does not trade positively for the mission as a whole, reducing the mission 1 endurance severely. This finding also implies that that there are two possible solutions yielding the same constrained optimum for the all-electric endurance. Designs

2 and 3 are precisely the other solution in this space. Including mission 1 endurance term in the objective function resulted in zeroing out the removable battery while maintaining the same all-electric endurance.

Table 5.1-1 Naming convention definition and weighting factor for each objective function type

Cases	Objective function	w_1	w_2	F
Case 1	F1	0	1	$F = -\left(\frac{E_2}{E_{req}}\right)$
Case 2	F1	1	0	$F = -\left(\frac{E_1}{E_{bl}}\right)$
Case 3	F1	0.5	0.5	$F = -0.5\left(\frac{E_1}{E_{bl}}\right) - 0.5\left(\frac{E_2}{E_{req}}\right)$
Case 4	F2	1	0	$F = -\left(\frac{ESAR_1}{ESAR_{bl}}\right)$
Case 5	F2	0.5	0.5	$F = -0.5\left(\frac{ESAR_1}{ESAR_{bl}}\right) - 0.5\left(\frac{E_2}{E_{req}}\right)$

The results for the baseline and the 5 cases are summarized below in Table 5.1-2

Table 5.1-2 Summary of the 6 design optimization cases for the hybrid electric UAV

Aircraft Parameter	Baseline	Design 1	Design 2	Design 3	Design 4	Design 5
PWR	0.0516	0.08	0.082	0.08	0.105	0.10
ϕ_{des}	0	0.38	0.382	0.38	0.545	0.53
$\phi_{climb,1}$	0	0.28	0.000	0.00	0.218	0.12
$\phi_{climb,2}$	0	0.00	0.000	0.00	0.160	0.09
Elec. Cruise RPM	--	4462	4462	4431	4462	4462
M1 Endurance Δ(%)	0 (40.3)	-58.83	-8.34	-8.34	-61.66	-38.11
M1 ESAR Δ(%)	0 (0.7223)	-12.54	-2.61	-2.61	-17.25	-11.93
M2 Endurance (hr)	0	0.455	0.458	0.458	0.130	0.280
ICE Power (hp)	115	114.0	113.4	113.4	107.2	103.3
Electric Motor Power (hp)	0	71.3	70.2	70.2	128.1	118.6
Climb Battery W (lbm)	0	329.8	0.0	0.0	320.3	161.3
All-Electric Battery W (lbm)	0	12.3	343.3	343.3	7.5	168.4

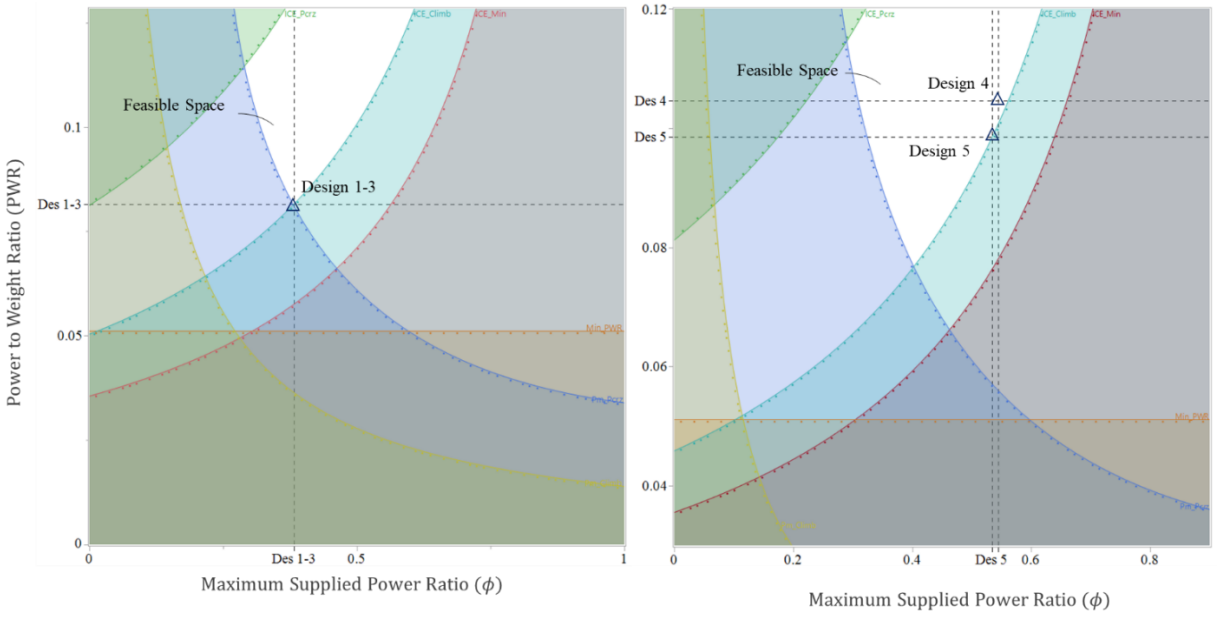

Figure 5.1-2 Multi-mission constraint space diagram showing all 6 designs optimized and the feasible space available in each case

Switching the objective function to F2, the optimizer converged to designs 4 and 5 with a higher supplied power ratio and overall level of power. Interestingly, the optimizer converged to a local optima at this large motor size that produces a worse ESAR for mission 1 and a smaller electric endurance. The conclusion is that some other optimization algorithm may be necessary to find global solutions in this space, or at least restarting the optimizer from different initial points may result in better solutions.

The solution space with the constraints can be visualized as shown in Figure 5.1-1. The minimum climb ICE power constraint (light green line) depends on the climb supplied power ratio for each mission, and is active in every case. For cases 1-3, the electric cruise constraint is active and the minimum motor power is selected to allow for all-electric cruise, while minimizing the empty weight increase. The intersection of these two constraint lines is the design point for cases 1-3. For cases 4 and 5, the electric motor is sized up to enable larger electric usage during climb, but as already discussed above, this case is not the global optimal solution for the F2 objective function.

5.2 Technology Sensitivity

A sensitivity analysis was conducted to assess impact of specific energy, which is a major technology parameter on the performance. The results in Figure 5.2-1 demonstrate that increasing specific energy increases the all-electric range, since there is more energy storage available within the weight limit. The electric motor sizing point remains constant as batteries improve. This implies that the boosted climb concept does not work very well regardless of energy density. This is most likely due to the propeller already operating near optimal speed during the cruise segment. In general, the main benefit of this system is the optional ability to perform all-electric cruise. However, the optimization technique developed here may help realize benefit for other UAV types where other benefits could be explored.

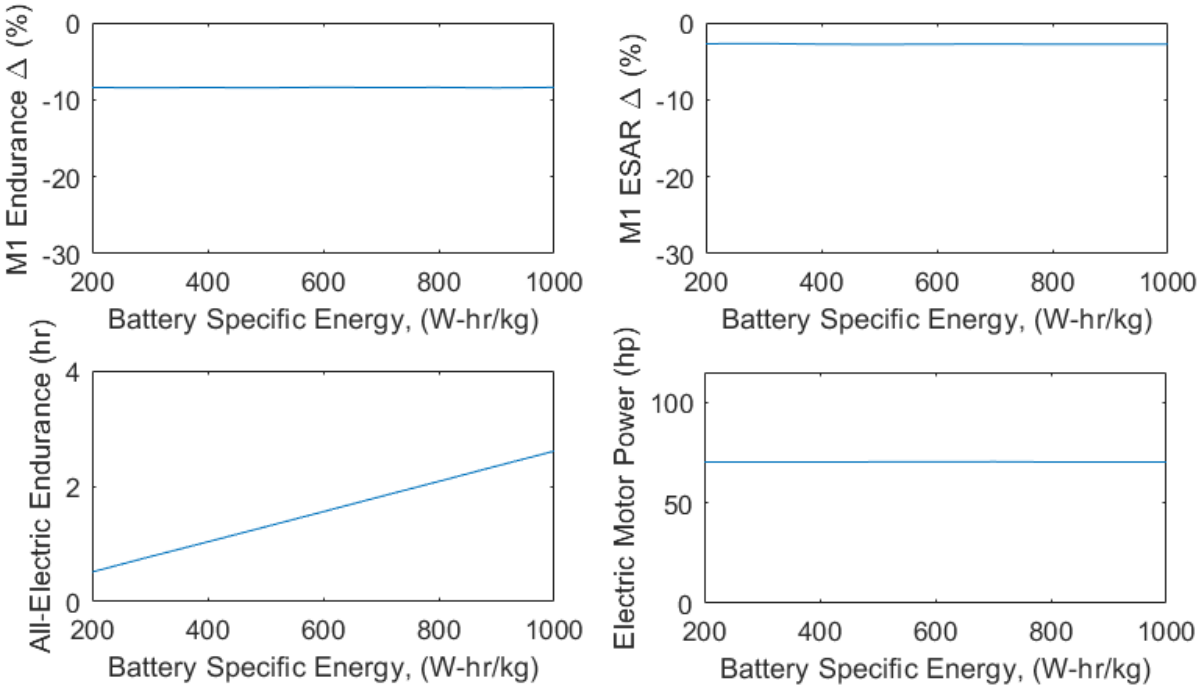

Figure 5.2-1 Optimization results (design variables and performance metrics) as a function of battery specific energy (200 – 1000 W-hr/kg) for the case with Mission1 endurance with a balanced objective function.

6.0 CONCLUSIONS

This paper has demonstrated a method for multi-mission conceptual optimization for hybrid electric aircraft with application to a long range reconnaissance UAV. While the method optimizes a specified objective function, it cannot guarantee the global optimal. An initial finding was that balanced objective functions tended to find the global solution easily.

Results indicate that an all-electric cruise is achievable for a reconnaissance UAV but this would inevitably reduce endurance or ESAR due to increased empty weight. Approximately half hour of all-electric cruise can be achieved at current energy densities and further improvements would improve the cruise endurance almost linearly. Though a boosted climb scenario was investigated by the optimization routine, it consistently found that no benefit could be achieved within the parameters of the design. Further research may be needed to determine whether performance can be improved either by re-optimizing the propeller design or selecting a smaller engine.

7.0 REFERENCES

[1] Aravindan, V., Gnanaraj, J., Lee, Y.S., and Madhavi, S. (2014), "Insertion-type Electrodes for Nonaqueous Li-Ion Capacitors ", Chemical Reviews.

[2] Ausserer, J. (2018), Integration, Testing, and Validation of a Small Hybrid-Electric Remotely-Piloted.

[3] DoD (2009), FY2009 – 2034 Unmanned Systems Integrated Roadmap", Department of Defense.

[4] Glassock, R., Hung, J. Y., Gonzalez, L. F., and Walker, R. A. (2008), Design, modelling and measurement of a hybrid powerplant for unmanned aerial systems, Australian Journal of Mechanical Engineering. doi: 10.1080/ 14484846.2008.11464559.

[5] Hamilton Standard (1961-1963), Generalized Method of Propeller Performance Estimation. Windsor Locks, CT, available at https://open.bu.edu/handle/2144/10454 (accessed on 1 June 2019).

[6] Harmon, F.G., Frank, A. A., and Chattot, J.J. (2006), Conceptual Design and Simulation of a Small Hybrid-Electric Unmanned Aerial Vehicle, Journal of Aircraft, 43(5):1490–1498. ISSN 0021-8669. doi: 10.2514/1.15816. URL http://arc.aiaa.org/doi/10.2514/1.15816.

[7] Pokhrel, M., Gladin, J. C., Ali, K., Collins, K., and Mavris, D. N. (2015), Modeling and Requirements Definition for a Hybrid-Electric Powered Helicopter, Proc. Of AHS Sustainability 2015, Montreal, Quebec, Canada

[8] Predator RQ-1 / MQ-1 / MQ-9 Reaper UAV", Air Force, available at https://www.airforce-technology.com/projects/predator-uav (accessed on 1 June 2019).

[9] Rotax 914 Aircraft Engine Datasheet", Rotax Aircraft Engines, available at https://www.flyrotax.com/files/Bilder/Produkte%20Rotax/Datasheets/Produktdatenblatt_914_115hp_rev.BRP-Rotax_20160823.pdf (accessed on 1 July 2019).

[10]UAV, General Atomics MQ-1L Predator A, Smithsonian National Air and Space Museum, available at https://airandspace.si.edu/collection-objects/uav-general-atomics-mq-1l-predator (accessed on 1 June 2019).